Chapter 15
Confocal and Transmission Electron Microscopy for Plant Studies

Adela M. Sánchez-Moreiras, Marianna Pacenza, Fabrizio Araniti, and Leonardo Bruno

1 Transmission Electron Microscopy

1.1 *The Significance of Structural and Ultra-Structural Studies*

The development of high-sensitive microscopic techniques, together with the development of methods for the conservation of cells and the improvement of methods for obtaining ultra-fine sections, gave rise to the knowledge of the cellular structure in the second half of the twentieth century. The combination of these techniques with immune-cytological techniques and the use of computational systems of image analysis have increased the interest in the use of electron and confocal microscopy in biological research. In fact, the use of transmission electron microscopy is very useful as a first approach for the characterization of the plant response to biotic or abiotic stress conditions. Knowing which areas of the cell morphology are being altered after treatment is essential to establish new physiological or biochemical measures for the in detail study of the effects of stressing factors on plants. A general view of the root or shoot tissues examined under microscopy will allow the identification of cellular organization, where alterations can be detected as erroneous division patterns, loss of cell identity or cellular disorganization (Rost et al. 1996; Zhu and Rost 2000). In particular, root tips act as finely tuned sensor for

A. M. Sánchez-Moreiras
Department of Plant Biology and Soil Science, University of Vigo, Vigo, Spain

M. Pacenza · L. Bruno (✉)
Department of Biology, Ecology and Earth Science, University of Calabria,
Arcavacata di Rende, CS, Italy
e-mail: leonardo.bruno@unical.it

F. Araniti
Department Agraria, Mediterranea University, Reggio Calabria, Italy

different kinds of stress, which makes their study especially interesting for interpreting the plant stress response (Colmer et al. 1994; Koyro 2002).

Root cells are generated, from a small number of stem cells at the apex of the root, by division and continuous cell expansion and differentiation, so that it is possible to find all stages of cell development at the same time (Scheres et al. 2002). Roots have four types of stem cells or initial cells (Dolan et al. 1993): (i) the initial cells of the lateral layer or of the epidermis of the root, which give rise to the epidermis and to the lateral layer; (ii) the central zone of the calyptra, the columella, which has its own initial cells; (iii) the vascular tissue and the pericycle, which also have their own initial cells; and, finally, (iv) the cortex and the endodermis, which are generated by divisions of the initial cells of the cortex and the endodermis (Scheres et al. 2002). Internally, and in contact with all these undifferentiated cells, is the quiescent center, a group of mitotically inactive cells that are responsible for maintaining the activity of the stem cells (Scheres et al. 2002). The initial cells of the columella divide only anticline (perpendicular to the axis of growth) giving rise to a single row of cells, and their progeny undergo rapid cell expansion and differentiation producing amyloplasts, which play a fundamental role in gravitropism. The other three initial cell types are divided by anticlinal and periclinal divisions (parallel to the growth axis) giving rise to several layers of cells that acquire different identities (Dolan et al. 1993). Any change on the division, expansion or differentiation of initial cells can lead to totally malformed tissues.

Transmission electron microscopy study allows obtaining information about the morphology, disposition and size of these cells and their cellular organelles, which are usually affected when plants are under stress. Moreover, ultra-structural changes induced by a specific type of stress are usually quite consistent among species, which gives an advantage for the interpretation of the relevance of biotic or abiotic stress impact. The most commonly affected cell parts are the nucleus, the mitochondria, the vacuoles and the chloroplasts in photosynthetic cells, although cell wall alterations and Golgi activity can also give essential information to get a whole picture of the cellular response to stress (Fig. 15.1).

1.1.1 Nucleus

Abiotic stress, as produced by toxins, metals, herbicides, pollutants, reactive oxygen species, deficit or excess water, high or low temperatures, salinity or high light, frequently results in the induction of cell death processes (Joseph and Jini 2010). Actually, programmed cell death can be part, under these conditions, of an adaptive mechanism to survive stress (Palavan-Unsal et al. 2005). Nuclei alterations, typical of apoptotic-like PCD (AL-PCD), such as chromatin condensation and DNA fragmentation, formation of herniae in the nuclear membrane or migration of the nucleus to the cellular periphery, have been found in presence of abiotic stress (Tao et al. 2000; Palavan-Unsal et al. 2005; Díaz-Tielas et al. 2012).

Besides PCD-related changes, nuclei can also show other alterations that will give interesting information about other kind of plant responses to stress; i.e. amorphous and irregular nuclei and bi- or multi-nucleate cells can be associated
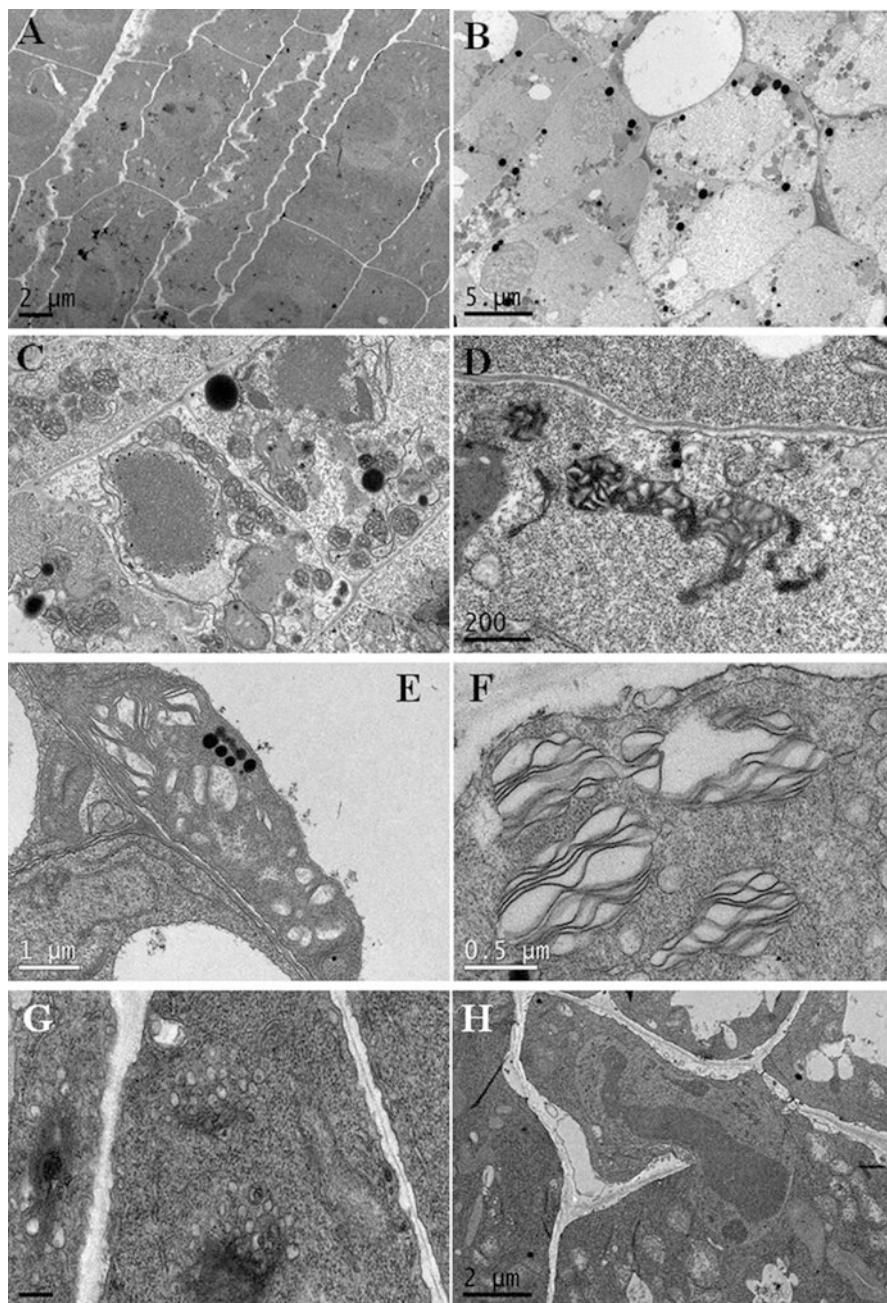
Fig. 15.1 TEM images of *Arabidopsis* treated cells. (**a**) Zigzag cell walls in citral-treated roots; (**b**) Disorganized and degraded cells in chalcone-treated roots; (**c**) Condensed mitochondria and distorted nuclei with nuclear membrane hernia and fragmented chromatin in chalcone-treated cells; (**d**) Condensed, irregular and broken mitochondria in chalcone-treated cell; (**e**–**f**) Swollen thylakoid in chalcone-treated shoots; (**g**) Increased Golgi-activity in eugenol-treated cells; (**h**) Incomplete cell wall formation in farnesene-treated cell

with cell wall malformations and, in particular, with erratically arranged microtubules (MTs), and shorter and fewer MTs in the arrays that can lead to aberrant chromosomal arrangements, misaligned or incomplete cell plates and distorted cell division (Kawamura et al. 2006; Araniti et al. 2016; Graña et al. 2017).

1.1.2 Mitochondria

Mitochondria play also a key role in AL-PCD response to stress, as apoptotic-like signal is usually initiated in these organelles. The intracellular machinery responsible for AL-PCD depends on the mitochondrial release of cytochrome c and other apoptogenic factors (Reape et al. 2008). Permeability transition pores are formed in the outer mitochondrial membrane, leading to a decrease in mitochondrial membrane potential or to the opening of a voltage-dependent anionic channel that results in the release of these apoptogenic factors from the space between the two mitochondrial membranes (Yao et al. 2004; Reape et al. 2008), which will lead to the cleavage of specific intracellular substrates that lead to cell death. Highly condensed and swollen mitochondria showing electron-dense matrix and a large number of cristae are typical of depolarized mitochondria involved in AL-PCD (Kiechle and Zhang 2002; Díaz-Tielas et al. 2012). Mitotic role in AL-PCD can include also the process of mitoptosis, which is the entry of mitochondria in the nucleus in which apoptogenic factors are released (Skulachev et al. 2004) and that has been previously shown for Arabidopsis stressed cells (Díaz-Tielas et al. 2012).

Increased number and size of mitochondria is also an interesting signal of plant response to stress. Peroxidation of mitochondrial membranes by ROS can result in membrane depolarization and irreversible loss of mitochondrial functions such as mitochondrial respiration, oxidative phosphorylation and ion transport (Vladimirov et al. 1980; Arpagaus et al. 2002), with the concomitant ATP deficit in the cell, which will increase mitochondrial number as a strategy of root cell to compensate mitochondrial dysfunction satisfying cellular energy requirements (Hardie 2011; Suksungworn et al. 2017; Araniti et al. 2016).

1.1.3 Chloroplasts

As key organelles in plant physiology due to the significance of photosynthesis for plant development, chloroplasts are one of the most common early target organelles of biotic and/or abiotic stress (Kratsch and Wise 2000; Giełwanowska et al. 2015; Díaz-Tielas et al. 2017). In particular, chloroplasts are especially susceptible to oxidative stress due to the high concentration of unsaturated fatty acids present in the thylakoids. Chloroplast swelling, thylakoid dilation and disintegration, plastoglobuli formation, reduced size and number of starch granules, unstacking of grana, intergranal vacuolation, disintegration of chloroplast envelope, darkening of the stroma and accumulation of lipid droplets, are among the most common changes observed in chloroplasts under cold, salinity, high light, herbicide, heavy metal,

high temperature, or drought stress (Kratsch and Wise 2000; Stefanowska et al. 2002; Zhang et al. 2010; Meng et al. 2016; Díaz-Tielas et al. 2017). Disruption of chloroplast ultra-structure is associated with an early detriment of photosynthesis affecting the correct development of plants.

1.1.4   Golgi, Vacuoles and Other Cellular Structures

The increase in the activity and number of Golgi complexes and endoplasmic reticulum has been related to active detoxification processes, since they participate in the release of secretory vesicles and in the synthesis of lipid globules (Kaur et al. 2005). Detoxified bioproducts are compartmentalized in vacuoles or deposited in the cell wall, which is usually related to an increase in the number of vacuoles and the presence of thickened cell walls. It has also been shown that treatment with compounds that inhibit mitochondrial respiration results in associations between the Golgi apparatus and the endoplasmic reticulum as a result of a decrease in vesicle production due to energy depletion (Robinson and Kristen 1982), in addition to changes in the morphology of the Golgi complex, which acquires a cup-shaped arrangement (Kandasamy and Kristen 1987).

Moreover, vacuolation has been previously related to PCD process in plant cells. In particular, the rupture and disappearance of large central vacuoles commonly found in healthy plant cells has been found to occur prior to the degradation of the nucleus and the programmed death of cells (Zheng et al. 2017). The protoplast of several vacuoles can also break and release its hydrolytic contents to the cytosol (Díaz-Tielas et al. 2012).

Finally, enlargement of the vacuoles has also been found as a response to salt, drought or chemical stress due to accumulation of proline and other osmolytes in the vacuole for osmotic adjustment (Patakas et al. 2002) or to the sequestration of cations, heavy metals or other undesired compounds (Sauge-Merle et al. 2003).

Other cellular structures, such as peroxisomes (Fahy et al. 2017); autophagosomes (Minibayeva et al. 2012; Araniti et al. 2016); amyloplasts (Graña et al. 2013); or ribosomes can be also altered or just appear/disappear under mild or severe plant stress.

1.1.5   Plant Cell Wall

Stressing factors can lead to the appearance of incomplete cell walls due to problems in the formation of the phragmoplast and alterations in its thickness (Hepler and Bonsignore 1990; Vaughn et al. 1996). In many cases, the underlying cause of these wall dysfunctions are problems in cytokinesis and formation of the phragmoplast for the physical separation of the cytoplasm during cell division, since a successful cytokinesis is essential not only for correct morphogenesis, but also for an appropriate architecture of the body of the plant (Verma 2001). Moreover, the

abnormal cell plates formed after microtubule disrupter can be enriched in callose thickening cell walls (Vaughn 2006).

Biosynthesis of wall polysaccharides shows enormous plasticity to several environmental factors (His et al. 2001), with different types of stress causing different balance of deposition of the different components, principally affecting the cellulose-xyloglucan network and compensating the reduction in cellulose content by increasing the pectin content (Burton et al. 2000; Aouar et al. 2010; Graña et al. 2013). Thickened and multilamellar cell walls with strong deposit content and irregularities in phragmoplast formation have been previously reported in plants under stress (García-Angulo et al. 2009; Graña et al. 2013; Araniti et al. 2016). Moreover, the thickening of the cell wall can greatly difficult the formation of plasmodesmata, impeding correct cell-cell communication and consequently causing the loss of tissue identity (Graña et al. 2013).

1.2   The Technique of Transmission Electron Microscopy (TEM)

Electron microscopy is mainly based on the observation under vacuum of fixed and dehydrated cellular and subcellular structures in stained ultrathin sections. The use of electron microscopy for the study of plant preparations started with the observation of isolated organelles (such as chloroplasts) and the visualization of cell walls (Roland and Vian 1991), mainly due to the difficulties that the presence of large vacuoles (soft compartments) and rigid cell walls (hard structures) represented in the preparation of electron microscopy sections from plant samples. Considering that the tonoplast (the membrane surrounding the vacuole) is highly sensitive to chemicals, strong care should be taken during the preparation of EM samples to avoid vacuole rupture and release of potentially damaging enzymes or compounds to the cytosol. Development of specific cytochemistry techniques, more specific reagents and a plurality of embedding materials allowed overpassing these difficulties and the heterogeneity of plant specimens and permitted to obtain high quality preparations. Although a slow and more complex microscopic technique, when compared to light or confocal microscopy, transmission electron microscopy (TEM) offers strong resolution and accuracy – to a resolution of 0.2 nm – when fine details are under study (Wilson and Bacic 2012).

Moreover, nowadays, we have new branches of transmission electron microscopy that enhance preparation and imaging of the samples; e.g. TEM tomography can generate semi-3D reconstructions (±60/70°) of plant cells and tissues at nanometer resolutions, while cryo-TEM allows visualization of frozen unstained samples (no reagents added during the process) avoiding alteration of ultrastructural details. TEM tomography and cryo-TEM can be coupled, although the necessity of sophisticated machinery strongly increases the cost of the preparations (Wilson and Bacic 2012).

There is no model recipe that can be used to prepare all kinds of plant tissues, therefore we show below a procedure to fix and stain root meristems or young shoots of *Arabidopsis* seedlings (Fig. 15.1). Meristematic zones are usually preferred, especially for beginners, when visualizing a sample due to the presence of smaller vacuoles and densely packed cytoplasm. When analyzing the effects of a treatment on cell ultra-structure, the numerical expression of morphological information (i.e. number of mitochondria, size of nuclei, number of autophagosomes, amount of swelling thylakoids, etc.) can be useful in the assessment of the effects of that treatment on cells, tissues and organs (Steer 1991).

1.3   Experimental Procedure for TEM Analyses

1. For roots: cut the apical meristem or the area of interest (1–2 mm) and introduce it immediately in 0.1 M cacodylate buffer (pH 7.2) until the fixation step
For shoots: cut the areas of interest of the living shoots into pieces of 1–2 mm, eliminate any superficial humidity and introduce them in an eppendorf tube (4–5 pieces per tube). Immediately after, fill the tubes with 0.1 M cacodylate buffer (pH 7.2), and introduce these tubes in a vacuum chamber for 15 min
2. Fix the root or shoot sample in 5% glutaraldehyde in 0.1 M cacodylate buffer (pH 7.2) at 4 °C for 4 h. To avoid artifacts or undesired modifications proceed as soon as possible with this step after sample excision
3. Wash in 0.1 M cacodylate buffer at 4 °C for 12 h (3 × 4 h)
4. After washing, incubate the samples in 2% osmium tetroxide in 0.1 M cacodylate buffer at 4 °C for 3 h
5. Incubate then in 2% uranyl acetate in 10% acetone at 4 °C for 1 h
6. Dehydrate with the following increasing acetone solutions (do all steps at 4 °C):
50% Acetone, 2 × 30 min
75% Acetone, 2 × 1 h[a]
80% Acetone, 2 × 1 h
95% Acetone, 2 × 1 h
100% Acetone, 2 × 2 h[b]
7. Infiltrate the sample in Spurr's resin at 4 °C as follows:
Spurr: acetone (1:3 v/v) (3 × 2 h)
Spurr: acetone (1:1 v/v) (3 × 2 h)[b]
Spurr: acetone (3:1 v/v) (2 × 2 h plus 1 × 3 h)
8. Embed the sample in 100% Spurr's resin for 2 × 3 h and left it overnight at room temperature
9. Embed the sample again in 100% resin (2 × 3 h)
10. Place the samples in pure resin in the molds and let them polymerize at 60 °C for 48 h
11. As the same fixation and embedding medium can be used for light and electron microscopy, check samples in semi-thin sections with light microscopy prior to continue with electron microscopy. For that, prepare semithin sections (0.7 μm) for light microscopy and then ultrathin sections (50–70 nm) for electron microscopy (ultrathin sections are mandatory to allow electrons correctly passing through the sample)

12. Contrast the samples as follows: incubate with uranyl acetate for 30 min; wash in boiled distilled water for 2 min; incubate with lead citrate for 10 min, and wash again in boiled distilled water for 2 min

13. Assemble ultrathin sections on copper grids of 100/200 mesh and examine by TEM using a JEOL JEM-1010 transmission electron microscope (at 100 kV) (Peabody, MA, USA) equipped with a CCD Orius-Digital Montage Plug-in camera (Gatan Inc., Gatan, CA, USA) and Gatan Digital Micrograph software (Gatan Inc.)

[a]The process can be stopped for a certain period
[b]It can stay overnight

2   Confocal Microscopy

The optical imaging technique based on confocal microscopy, also known as confocal laser scanning microscopy, aims to increase both contrast and optical resolution of a given sample micrograph using a spatial pinhole that blocks out-of-focus light during the formation of images (Matsumoto 2003). Unlike conventional microscopy, where the light passes through the sample, as far as it can penetrate, in confocal microscopy a beam of light is focused at one narrow depth level at a time. This technique, achieving a controlled and highly limited depth of focus, allows the reconstruction of 3D structures, of both biological and non-biological samples, through the acquisition at different depths of multiple two-dimensional images that are successively elaborated by a software (Matsumoto 2003). The ability to recreate three-dimensional images of microscopic samples allowed its diffusion in several research fields such as material science, semiconductor inspection and life science (Bruchez et al. 1998; Cardinale 2014; He et al. 2015; Fuchs et al. 2015; Bertani et al. 2017; Ben-Tov et al. 2018).

Concerning life science, confocal microscopy has revolutionized our knowledge about cells. It has became a pivotal tool for imaging both cell function and structure as well as the complexities of the morphology and dynamics of single cells and entire tissues (Amin et al. 2017). Moreover, since confocal microscope optically sections the specimen in a relatively non-invasive manner, it can be used to observe fixed as well as living samples increasing the potential of this technique in the understanding of several molecular and physiological dynamics (Araniti et al. 2017; Luo and Russinova 2017; Dinh et al. 2018).

In the past, the research through confocal microscopy was mainly focused on the study of cell structure and on the observation of spatial distribution of the organelles, whereas nowadays scientists continuously try to push to its limits confocal technology. For example, Shargil et al. (2015) have been able to detect and localize the cucumber green mottle mosaic virus (CGMMV) in both vegetative and reproductive tissues of cucumber and melon through in-situ hybridization technique. In particular, they observed that all tissues were infected by the virus, whereas the

pollen was virus-free, highlighting that virulence transmission was mainly due to vectors such as insect instead of gamic transmission.

Zhao et al. (2012), studying soils contaminated with zinc oxide and nanoparticles demonstrated that both zinc oxide and nanoparticles penetrate root epidermis and cortex through the apoplastic way, whereas penetrate endodermis through the symplast. In addition, confocal microscopy technique has been largely used to study both plant nutrition and signaling in plants, and ion fluxes propagation could be followed through both entire living cells and tissues (Larrieu et al. 2015; Tian et al. 2016). For example, recent studies demonstrated that plants are able to quickly activate a signaling system based on Ca^{2+} waves that propagate in plant through the cortex and endodermal cell layers. In particular, it has been observed that Ca^{2+} movement depends on the vacuolar ion channel TPC1 and this Ca^{2+}/TCP1 system, eliciting specific responses in target organs, could contribute to increased stress-tolerance by whole plant (Choi et al. 2014).

Nowadays, there are available on the market probes for any kind of research activity, and this technological development has opened a new world to scientists interested in the dynamic complexities of cells and tissues (Wiederschain 2011). For example, the fluorescent labeled actin is a probe largely used to investigate the structural dynamics of the cytoskeleton (Araniti et al. 2016; Vaškebová et al. 2017), whereas Mito-Traker, Er-Traker, Bodi-Py ceramide, Lyso-Traker and DAPI probes are used to stain cellular organelle such as mitochondria, endoplasmic reticulum, Golgi complex, lysosomes and nuclei, respectively (Wiederschain 2011; Zhou et al. 2014; Chen and Zhang 2015; Chumak et al. 2015; Lee and Back 2017; Ibl et al. 2018). Fluorophores for probing cell function and structure (from ion flux to cell viability and from organelles and membrane to whole cells), for detecting biomolecules, for detecting and localizing oxidative stress, etc., are largely available and they have a contained cost considering the information they give (Wiederschain 2011).

Nowadays, using a chimeric fluorescent protein as an endogenous probe, such as GFP (green fluorescent protein), YFP (yellow fluorescent protein), etc., labeled proteins can be expressed within cells (specific tissues organelle and entire tissues) (Chalfie et al. 1994). Indicator molecules, which change their fluorescent characteristics as they sense changes in hormones concentration, pH, ions concentration, membrane potential etc., have been introduced into model species (e.g. *Arabidopsis thaliana*) and their mutants allowing to optically monitor the physiological state and its changes of entire tissues, as well as of individual cells (D'Angelo et al. 2006; Monshausen et al. 2007; Liu et al. 2015; Liu and Müller 2017). For example, Araniti et al. (2017) used several PIN*s*::GFP mutants to identify the mode of action of the natural compound farnesene, whereas Bruno et al. (2017) demonstrated that cadmium impacted growth of Arabidopsis primary root, altering auxin-cytokinin crosstalk and scarecrow expression. Those results highlight the potential of confocal microscopy, which is a robust and versatile technique with a variety of fields of application.

Two confocal microscopy techniques used to evaluate Arabidopsis root anatomy and protein immune-localization will be described below.

2.1   mPS-PI Staining

The use of sections obtained by cutting embedded tissues into paraffin blocks or resin and mounted onto microscope slides is always been the method of choice for the observation and the study, in plants, of the organization of tissues and their cells (Fig. 15.2).

Thanks to the advent of confocal microscopy (CLSM, Confocal Laser Scanner Microscopy), it became possible to obtain optical sections of the tissues without having to resort to actual sectioning of the samples, which implies a substantial reduction of the workload and, consequently, of the experimental timing. Moreover, the CLSM allows collection of sequential images on z-axis thanks to the use of specific software, and the subsequent reconstruction 3D of the samples. Unfortunately, the use of confocal microscopy on fresh samples is limited to thin and semi-transparent organs, like roots of seedlings of *Arabidopsis thaliana* (Helariutta et al. 2000; Kurup et al. 2005; Laplaze et al. 2005; Stadler et al. 2005).

Fig. 15.2 Confocal laser image of primary root tip in *Arabidopsis thaliana* seedling at 7 days after germination (DAG), stained by using mPS-staining protocol (Truernit et al. 2008). *cl* columella, *c* cortex, *en* endodermis, *ep* epidermis, *M* meristematic zone, *pl* cap peripheral layers, *qc* quiescent center, *s* stele, *TZ* transition zone. Scale bar 46 μm
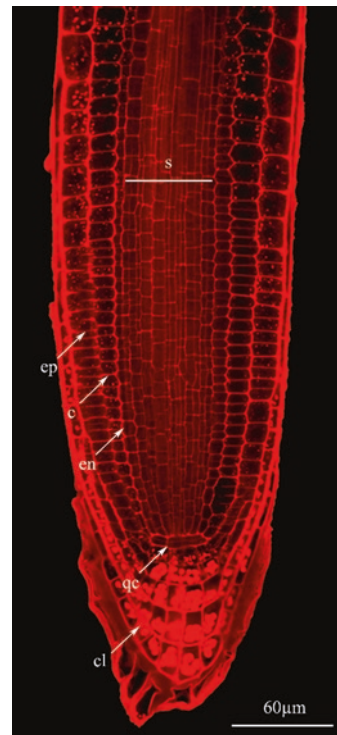
In fact, the presence in the aerial parts of plants of substances suitable to prevent the excessive penetration of light radiation, in addition to the presence of cell walls, cause spherical aberrations and dispersion of the luminous laser beam of the microscope, preventing penetration through the sample. These factors compromise the quality of the final images, especially during the observation of deeper layers of tissues (from ≥50 to 100 μm) (Haseloff 2003; Moreno et al. 2006).

To obtain optimal results in the observation of deeper layers of tissues ($0.3 \times 0.3 \times 0.5$ μm) by using confocal microscopy, it is therefore advisable to resort to the use of clarifying agents with high refractive indexes on correctly fixed samples (Truernit et al. 2008). The mPS-PI (Pseudo-Schiff Propidium Iodide) staining technique, published by Truernit et al. (2008), allows obtaining, in relatively short times, high-resolution images at cellular level of *Arabidopsis thaliana* tissues, in all organs and in all developmental stages. The staining is based on aldehyde groups' creation in cell walls carbohydrates of the samples following periodic acid treatment. These aldehyde groups, later, react covalently with pseudo-Schiff reagents such as propidium iodide. The formation of these covalent bonds on the walls makes them highly fluorescent, allowing the analysis of tissues at the cellular level through confocal microscopy in a detailed manner (Truernit et al. 2008). This method can also be combined with gene expression studies using β-glucuronidase (GUS).

2.1.1 Materials

– Distilled water;
– Methanol (CH_4O; CAS 67-56-1; FW 32.04);
– Acetic acid (CH_3COOH; CAS 64-19-7; FW 60.05);
– Ethanol (C_2H_6O; CAS 64-17-5; FW 46.07);
– Periodic Acid (HIO_4; CAS 10450-60-9; FW 227.94);
– Sodium metabisulphite ($Na_2S_2O_5$; CAS 7681-57-4; FW 190.10);
– Chloridric acid (HCl; CAS 7647-01-0; FW 36.46);
– Propidium iodide ($C_{27}H_{34}I_2N_4$; CAS 25535-16-4; FW 668.39);
– Chloral hydrate ($C_2H_3Cl_3O_2$; CAS 302-17-0; FW 165.40);
– Sodium dodecyl sulfate (SDS) ($NaC_{12}H_{25}SO4$; CAS 151-21-3; FW 288.37);
– Sodium hydroxide (NaOH; CAS 1310-73-2; FW 39.99);
– Arabic gum (CAS 9000-01-5; FW).

2.1.2 Experimental Protocol

1. Fix the samples in the fixative (50% methanol, 10% acetic acid in distilled water), making sure that they are completely covered, at 4 °C for at least 12 h. The samples can thus be stored in the fixative up to a month.
2. Transfer the tissue in 80% (v/v) ethanol and incubate at 80 °C from 1 to 5 min, depending on the type of tissue (example: 1 min for leaves, 5 min for flower stems).

Ethanol treatment is important to increase the efficiency of staining in some organs. As far as root and root primordial staining is concerned, the step with ethanol can be omitted, while in ovules and seeds staining this step is replaced by overnight treatment of the samples with 1% SDS and 0.2 N NaOH at room temperature (RT), followed by washing in water and incubation in 25% bleach solution (2.5% of Cl^- active) from 1 to 5 min. Then, perform another washing in water and proceed with treatment with 1% periodic acid (w/v) (point 4).

3. Transfer samples in fixative and incubate at RT for 1 h.
4. Wash samples in distilled water and incubate in 1% periodic acid (w/v) at RT for 40 min.
5. Wash samples in distilled water.
6. Prepare Schiff's reagent (100 mM sodium metabisulphite, 0.15 N HCl in distilled water), and freshly add the propidium iodide to the final concentration of $100 \, \mu g \, mL^{-1}$. Incubate the samples with Schiff's reagent at RT in the dark until the samples are visibly stained (around 2 h).
7. Transfer samples on slides and cover them with chloral hydrate solution (4 g chloral hydrate, 1 mL glycerol and 2 mL water).
8. Keep the slides overnight at RT in a closed container, to prevent them from drying out.
9. Remove the excess of chloral hydrate solution and coat the samples with Hoyer solution (30 g Arabic gum, 200 g chloral hydrate, 20 g glycerol and 50 mL water).
10. Cover the samples with the coverslip and allow them to stabilize for at least 3 days before the observation with a confocal microscope (excitation wavelength: 488 nm; reflection signal between 520 and 720 nm).

2.2 Whole Mount Immunolocalization in Plant

Despite the enormous progresses achieved in recent years in gene expression analyses, which allow to define the expression patterns of entire pathways in short times within plant (the so-called high-throughput techniques), in some cases, the in-situ localization of proteins at the cellular and sub-cellular level is still today the most efficient method for the study of functions, mechanisms of action and possible interactions between proteins and/or other cellular components.

Direct visualization by using recombinant DNA techniques with Green Fluorescent Protein (GFP) is one of the most used techniques for *in situ* localization of proteins, for its high reproducibility and the very short experimental times required for observation once obtained the specific construct for the proteins of interest; however, this approach in some cases does not accurately reflect the localization of the wild type (non-recombinant) protein, since the molecular properties of the recombinant protein are altered by GFP presence. In these cases, if the specific antibody is available, it is possible to resort to the immunolocalization of endogenous proteins (Sauer et al. 2006).
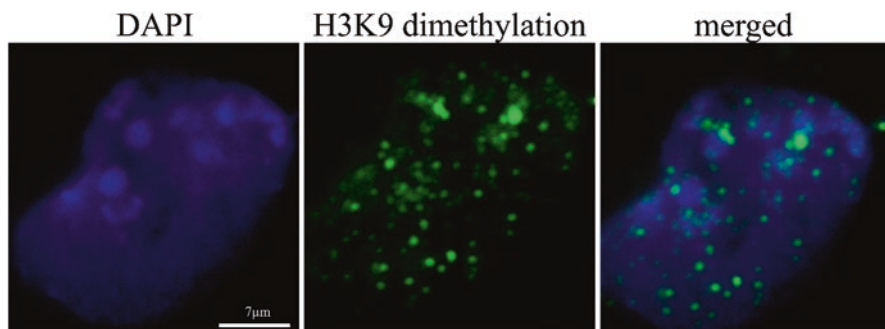
Fig. 15.3 Immunolocalization of histone H3 dimethylation at lysine position 9 on nuclei of the primary root of *Arabidopsis thaliana* seedlings growth at 8 days after germination (DAG)

In literature, there are many immunolocalization methods suitable for plants, however these methods require a prior work of inclusion and dissection of the tissues of interest, which makes them very laborious and unsuitable for a large number of samples, due to the large amount of time required to produce the necessary sections. One of the quickest and best performing methods is the one published by Sauer et al. (2006), which uses whole mount samples. A slightly modified version of this protocol is proposed here. This technique was optimized for *Arabidopsis thaliana* (Fig. 15.3), but good results were also obtained using the roots of tobacco plants (*Nicotiana tabacum*) and tomatoes (*Lycopersicon esculentum*).

The protocol consists of five main steps: (1) Tissue fixation, (2) Tissue permeation, (3) Incubation with the primary antibody, (4) Incubation with the secondary antibody, (5) Staining with DAPI (optional).

2.2.1 Materials

– Distilled water
– Potassium chloride (KCl; CAS 7447-40-7; FW 74.55)
– Sodium chloride (NaCl; CAS 7647-14-5; FW 58.44)
– Sodium phosphate dibasic dihydrate ($Na_2HPO_4 \cdot 2H_2O$; CAS 10028-24-7; FW 177.99)
– Potassium dihydrogen phosphate (KH_2PO_4; CAS 7778-77-0; FW 136.09)
– 1.4-Piperazinediethanesulfonic acid (PIPES; $C_8H_{18}N_2O_6S_2$; CAS 5625-37-6; FW 302.37)
– Ethylene glycol diacetate (EGTA; $HOCH_2CH_2OH$; CAS 107-21-1; FW 62.07)
– Magnesium sulfate heptahydrate ($MgSO_4 \cdot 7 H_2O$; CAS 7487-88-9; FW 120.37)
– Potassium hydroxide (KOH; CAS 1310-58-3; FW 56.11)
– Paraformaldehyde ($HO(CH_2O)_nH$; CAS 30525-89-4; FW 30.03 (monomer))
– Triton X-100 (-Oct-C_6H_4-$(OCH_2CH_2)_x OH$ x=9-10; CAS 9002931)
– Driselase (CAS 85186-71-6; EC number: 286-055-3)
– IGEPAL CA-630 (($C_2H_4O)_nC_{14}H_{22}O$; CAS 9002-93-1)

- Dimethyl sulfoxide (DMSO; $(CH_3)_2SO$; CAS 67-68-5; FW 78.13)
- Bovine serum albumin (BSA; CAS 9048-46-8; EC number 232-936-2)
- Primary antibody
- Secondary antibody
- Polyvinyl alcohol mounting medium with DABCO, antifading ($[-CH_2CHOH-]_n$).

  To detect proteins in hypocotyls. Cotyledons or young leaves:

- Methanol (CH_4O; CAS 67-56-1; FW 32.04);
- Ethanol (C_2H_6O; CAS 64-17-5; FW 46.07);
- Xylene (C_8H_{10}; CAS 1330-20-7; FW 106.16).

  Optional:

- 4′,6-Diamidino-2-phenylindole dihydrochloride (DAPI; $C_{16}H_{15}N_5 \cdot 2HCl$; CAS 28718-90-3; FW 350.25).

2.2.2   Experimental Protocol

Prepare the phosphate-buffered saline (PBS) or the microtubule-stabilizing buffer (MTSB).

10X PBS: Weigh and add 2 g KCl, 80 g NaCl, 17.8 g $Na_2HPO_4 \cdot 2 H_2O$ and 2.4 g KH_2PO_4 in one liter solution. After diluting 10X PBS with water to obtain 1X PBS, adjust pH to 7.4 with the addition of KOH.

1X MTSB: 15 g PIPES, 1.9 g EGTA, 1.32 g $MgSO_4 \cdot 7 H_2O$, 5 g KOH in one liter solution. If necessary, adjust pH to 6.8–7.0 with KOH.

1. Fix the samples in the fixative (4% paraformaldehyde, 0.1% Triton X-100 in 1X PBS). It is advisable to collect the ovules with the embryos in ice, since this operation takes a long time.
2. Incubate the samples in a vacuum pump with desiccator for 1 h at RT. For coriaceous organs, such as hypocotyls, it is recommended to prolong the treatment in order to guarantee the penetration of the fixative into the tissues.
3. Remove the fixative and perform two washes with 1X PBS for 5–10 min at RT.
4. To detect proteins in root apexes, in lateral roots and in embryos, go directly to point 5.

   To detect proteins in hypocotyls, cotyledons or young leaves:

   (a) Remove the 1X PBS and wash in methanol for 10 min at 37 °C. Repeat this wash if necessary until the chlorophyll is completely removed.
   (b) Remove the methanol and incubate the samples with a solution of 50% ethanol and 50% xylene for 10 min at 37 °C. Repeat this wash twice.

   (c) Remove the ethanol and xylene solution and incubate the samples in xylene for 10 min at 37 °C. Repeat this wash twice.

   (d) Remove xylene and incubate samples with a 50% ethanol and 50% xylene solution for 10 min at RT. Repeat this wash once.

   (e) Remove the ethanol and xylene solution and incubate the samples in absolute ethanol for 10 min at RT. Repeat this wash once.

   (f) Remove ethanol and incubate with 90% ethanol in 1X PBS for 5 min at RT.

   (g) Remove ethanol and incubate with 75% ethanol in 1X PBS for 5 min at RT.

   (h) Remove ethanol and incubate with 50% ethanol in 1X PBS for 5 min at RT.

   (i) Remove ethanol and incubate with 25% ethanol in 1X PBS for 5 min at RT.

5. Remove the liquid and wash twice with distilled water for 5 min at RT.
6. Incubate samples with 2% Driselase in 1X PBS at 37 °C for 30–60 min.
7. Remove the Driselase and perform six washes with 1X PBS for 5–10 min at RT.
8. Incubate the samples with 3% IGEPAL CA-630 and 10% DMSO in 1X PBS.
9. Remove the IGEPAL CA-630 and DMSO solution and perform five to ten washes with 1X PBS for 5–10 min at RT.
10. Incubate the samples with 3% BSA in 1X PBS for 60 min at RT.
11. Remove the BSA solution and incubate the samples with the solution containing the primary antibody (2% BSA in 1X PBS, the concentration of primary antibody must be determined experimentally) for at least 4 h at 37 °C. Incubation with the primary antibody can be prolonged overnight at 4 °C.
12. Remove the primary antibody and perform six washes with 1X PBS at RT.
13. Remove the 1X PBS and incubate the samples with the secondary antibody (2% BSA in 1X PBS, the recommended secondary antibody concentration ranges from 1: 600 to 1: 2000, but concentration may need to be optimized) for at least 3 h at 37 °C.
14. Remove the secondary antibody and perform six washes with 1X PBS at RT.
15. Prepare the DAPI stock solution (1 mg mL^{-1} DAPI in 1X PBS) (optional).
16. Prepare the DAPI solution (by diluting the DAPI stock solution in water at a concentration of 1: 1000) and incubate the samples for 30 min at RT (optional).
17. Remove the DAPI solution and perform four washes with distilled water for 10 min at RT (optional).
18. Remove the water, mount the samples on the slides with a drop of antifade mounting medium and cover the samples with a coverslip.
19. Observe samples under a confocal microscope or store slides at 4 °C in the dark to preserve fluorescence. Depending on the type of fluorophore used, the samples can be preserved from few days to weeks after staining.

References

Amin MA, Nandi S, Mondal P, Mahata T, Ghosh S, Bhattacharyya K (2017) Physical chemistry in a single live cell: confocal microscopy. Phys Chem Chem Phys 19:12620–12627

Aouar L, Chebli Y, Geitmann A (2010) Morphogenesis of complex plant cell shapes: the mechanical role of crystalline cellulose in growing pollen tubes. Sex Plant Reprod 23:15–27

Araniti F, Graña E, Krasuska U, Bogatek R, Reigosa MJ, Abenavoli MR, Sánchez-Moreiras AM (2016) Loss of gravitropism in farnesene-treated arabidopsis is due to microtubule malformations related to hormonal and ROS unbalance. PloS one 11(8):e0160202

Araniti F, Bruno L, Sunseri F, Pacenza M, Forgione I, Bitonti MB, Abenavoli MR (2017) The allelochemical farnesene affects *Arabidopsis thaliana* root meristem altering auxin distribution. Plant Physiol Biochem 121:14–20

Arpagaus S, Rawyler A, Braendle R (2002) Occurrence and characteristics of the mitochondrial permeability transition in plants. J Biol Chem 277:1780–1787

Ben-Tov D, Idan-Molakandov A, Hugger A, Ben-Shlush I, Günl M, Yang B, Usadel B, Harpaz-Saad S (2018) The role of COBRA-LIKE 2 function, as part of the complex network of interacting pathways regulating Arabidopsis seed mucilage polysaccharide matrix organization. Plant J 94(3):497–512. https://doi.org/10.1111/tpj.13871

Bertani FR, Mozetic P, Fioramonti M, Iuliani M, Ribelli G, Pantano F, Santini D, Tonini G, Trombetta M, Businaro L, Selci S, Rainer A (2017) Classification of M1/M2-polarized human macrophages by label-free hyperspectral reflectance confocal microscopy and multivariate analysis. Sci Rep 7:8965

Bruchez M, Moronne M, Gin P, Weiss S, Alivisatos AP (1998) Semiconductor nanocrystals as fluorescent biological labels. Science 281:2013–2016

Bruno L, Pacenza M, Forgione I, Lamerton LR, Greco M, Chiappetta A, Bitonti MB (2017) In *Arabidopsis thaliana* cadmium impact on the growth of primary root by altering SCR expression and auxin-cytokinin cross-talk. Front Plant Sci 8:1323

Burton RA, Gibeaut DM, Bacic A, Findlay K, Roberts K, Hamilton A, Baulcombe DC, Fincher GB (2000) Virusinduced silencing of a plant cellulose synthase gene. Plant Cell 12:691–706

Cardinale M (2014) Scanning a microhabitat: plant-microbe interactions revealed by confocal laser microscopy. Front Microbiol 5:94

Chalfie M, Tu Y, Euskirchen G, Ward WW, Prasher DC (1994) Green fluorescent protein as a marker for gene expression. Science 263:802–805

Chen H, Zhang X (2015) Subcellular localization of CAX proteins in plants. Mol Soil Biol 6:1–5

Choi W-G, Toyota M, Kim S-H, Hilleary R, Gilroy S (2014) Salt stress-induced Ca^{2+} waves are associated with rapid, long-distance root-to-shoot signaling in plants. PNAS 111:6497–6502

Chumak N, Mosiolek M, Schoft VK (2015) Sample preparation and fractionation of *Arabidopsis thaliana* sperm and vegetative cell nuclei by FACS. Bio Protocol 5(22):e1664

Colmer TD, Fan TWM, Higashi RM, Läuchli A (1994) Interactions of Ca^{2+} and NaCl stress on the relations and intracellular pH of *Sorghum bicolor* root tips. An in vivo ^{32}P-NMR study. J Exp Bot 45:1037–1044

D'Angelo C, Weinl S, Batistic O, Pandey GK, Cheong YH, Schültke S, Albrecht V, Ehlert B, Schulz B, Harter K, Luan S, Bock R, Kudla J (2006) Alternative complex formation of the Ca^{2+}-regulated protein kinase CIPK1 controls abscisic acid-dependent and independent stress responses in Arabidopsis. Plant J 48:857–872

Díaz-Tielas C, Graña E, Sotelo T, Reigosa MJ, Sánchez-Moreiras AM (2012) The natural compound trans-chalcone induces programmed cell death in *Arabidopsis thaliana* roots. Plant Cell Environ 35:1500–1517

Díaz-Tielas C, Graña E, Maffei M, Reigosa MJ, Sánchez-Moreiras AM (2017) Plasma membrane depolarization precedes photosynthesis damage and long-term leaf bleaching in (*E*)-chalcone-treated *Arabidopsis* shoots. J Plant Physiol 218:56–65

Dinh N, van der Ent A, Mulligan DR, Nguyen AV (2018) Zinc and lead accumulation characteristics and in vivo distribution of Zn^{2+} in the hyperaccumulator *Noccaea caerulescens* elucidated with fluorescent probes and laser confocal microscopy. Environ Exp Bot 147:1–12

Dolan L, Janmaat K, Willemsen V, Linstead P, Poethig S, Roberts K, Scheres B (1993) Cellular organization of the *Arabidopsis thaliana* root. Development 119:71–84

Fahy D, Sanad MNME, Duscha K, Lyons M, Liu F, Bozhkov P, Kunz H-H, Hu J, Neuhaus HE, Steel PG, Smertenko A (2017) Impact of salt stress, cell death, and autophagy on peroxisomes: quantitative and morphological analyses using small fluorescent probe N-BODIPY. Sci Rep 7:39069

Fuchs N, Krajewski P, Bernhard C (2015) In situ observation of austenite grain growth in plain carbon steels by means of high-temperature laser scanning confocal microscopy. BHM Berg- und Hüttenmännische Monatshefte 160:214–220

Giełwanowska I, Pastorczyk M, Kellmann-Sopyła W, Górniak D, Górecki RJ (2015) Morphological and ultrastructural changes of organelles in leaf mesophyll cells of the arctic and antarctic plants of Poaceae family under cold influence. Arct Antarct Alp Res 47:17–25

Graña E, Sotelo T, Díaz-Tielas C, Araniti F, Krasuska U, Bogatek R, Reigosa MJ, Sánchez-Moreiras AM (2013) Citral induces auxin-mediated malformations and arrests cell division in *Arabidopsis thaliana* roots. J Chem Ecol 39:271–282

Graña E, Costas-Gil A, Longueira S, Celeiro M, Teijeira M, Reigosa MJ, Sánchez-Moreiras AM (2017) Auxin-like effects of the natural coumarin scopoletin on Arabidopsis cell structure and morphology. J Plant Physiol 218:45–55

Hardie G (2011) AMP-activated protein kinase—an energy sensor that regulates all aspects of cell function. Genes Dev 25:1895–1908

Haseloff J (2003) Old botanical techniques for new microscopes. Biotechniques 34:1174–1183

He YM, Clark G, Schaibley JR, He Y, Chen MG, Wie YJ, Ding X, Zhang Q, Yao W, Xu X, Lu CY, Pan JW (2015) Single quantum emitters in monolayer semiconductors. Nat Nanotechnol 10:497

Helariutta Y, Fukaki H, Wysocka-Diller J, Nakajima K, Jung J, Sena G, Hauser MT, Benfey PN (2000) The SHORT-ROOT gene controls radial patterning of the Arabidopsis root through radial signaling. Cell 101:555–567

Hepler PK, Bonsignore CL (1990) Caffeine inhibition of cytokinesis: ultrastructure of cell plate formation/degradation. Protoplasma 157:182–192

His I, Driouich A, Nicol F, Jauneau A, Höfte H (2001) Altered pectin composition in primary walls of Korrigan, a dwarf mutant of Arabidopsis deficient in membrane-bound endo-1,4-β-glucanase. Planta 212:348–358

Ibl V, Peters J, Stöger E, Arcalís E (2018) Imaging the ER and endomembrane system in cereal endosperm. In: Hawes C, Kriechbaumer V (eds) The plant endoplasmic reticulum, Methods in Molecular Biology, vol 1691. Humana Press, New York, pp 251–262

Joseph B, Jini D (2010) Salinity induced programmed cell death in plants: challenges and opportunities for salt-tolerant plants. J Plant Sci 5:376–390

Kandasamy MK, Kristen U (1987) Pentachlorophenol affects mitochondria and induces formation of Golgi apparatus-endoplasmic reticulum hybrids in tobacco pollen tubes. Protoplasma 141:112–120

Kaur H, Inderjit, Kaushik S (2005) Cellular evidence of allelopathic interference of benzoic acid to mustard (*Brassica juncea* L.) seedling growth. Plant Physiol Biochem 43:77–81

Kawamura E, Himmelspach R, Rashbrooke MC, Whittington AT, Gale KR, Collings DA, Wasteneys GO (2006) MICROTUBULE ORGANIZATION 1 regulates structure and function of microtubule arrays during mitosis and cytokinesis in the Arabidopsis root. Plant Physiol 140:102–114

Kiechle FL, Zhang X (2002) Apoptosis: biochemical aspects and clinical implications. Clin Chim Acta 326:27–45

Koyro HW (2002) Ultrastructural effects of salinity in higher plants. In: Läuchli A, Lüttge U (eds) Salinity: environment – plants – molecules. Springer, Dordrecht, pp 139–157

Kratsch HA, Wise RR (2000) The ultra structure of chilling stress. Plant Cell Environ 23:337–350

Kurup S, Runions J, Köhler U, Laplaze L, Hodge S, Haseloff J (2005) Marking cell lineages in living tissues. Plant J 42:444–453

Laplaze L, Parizot B, Baker A, Ricaud L, Martiniere A, Auguy F, Franch C, Nussaume L, Bogusz D, Haseloff J (2005) GAL4-GFP enhancer trap lines for genetic manipulation of lateral root development in *Arabidopsis thaliana*. J Exp Bot 56:2433–2442

Larrieu A, Champion A, Legrand J, Lavenus J, Mast D, Brunoud G, Oh J, Guyomarc'h S, Pizot M, Farmer EE, Turnbull C, Vernoux T, Bennett MJ, Laplaze L (2015) A fluorescent hormone biosensor reveals the dynamics of jasmonate signalling in plants. Nat Commun 6:6043

Lee H-Y, Back K (2017) Cadmium disrupts subcellular organelles, including chloroplasts, resulting in melatonin induction in plants. Molecules 22:1791

Liu J, Müller B (2017) Imaging TCSn::GFP, a synthetic cytokinin reporter. In: Kleine-Vehn J, Sauer M (eds) *Arabidopsis thaliana*, Plant Hormones. Methods in Molecular Biology, vol 497. Humana Press, New York, pp 81–90

Liu J, Yang L, Luan M, Wang Y, Zhang C, Zhang B, Shi J, Zhao F, Lan W, Luan S (2015) A vacuolar phosphate transporter essential for phosphate homeostasis in Arabidopsis. PNAS 112:E6571–E6578

Luo Y, Russinova E (2017) Quantitative microscopic analysis of plasma membrane receptor dynamics in living plant cells. In: Russinova E, Caño-Delgado A (eds) Brassinosteroids, Methods in Molecular Biology, vol 1564. Humana Press, New York, pp 121–132

Matsumoto B (2003) Cell biological applications of confocal microscopy, vol 70. Academic, Cambridge, MA

Meng F, Luo Q, Wang Q, Zhang X, Qi Z, Xu F, Lei X, Cao Y, Chow WS, Sun G (2016) Physiological and proteomic responses to salt stress in chloroplasts of diploid and tetraploid black locust (*Robinia pseudoacacia* L.). Sci Rep 6:23098

Minibayeva F, Dmitrieva S, Ponomareva A, Ryabovol V (2012) Oxidative stress-induced autophagy in plants: the role of mitochondria. Plant Physiol Biochem 59:11–19

Monshausen G, Bibikova T, Messerli M, Shi C, Gilroy S (2007) Oscillations in extracellular pH and reactive oxygen species modulate tip growth of Arabidopsis root hairs. PNAS 104:20996–21001

Moreno N, Bougourd S, Haseloff J, Feijó JA (2006) Imaging plant cells. In: Pawley J (ed) Handbook of biological confocal microscopy. Springer, Boston, pp 769–787

Palavan-Unsal N, Buyuktuncer ED, Tufekci MA (2005) Programmed cell death in plants. J Cell Mol Biol 4:9–23

Patakas A, Nikolaou N, Zioziou E, Radoglou K, Noitsakis B (2002) The role of organic solute and ion accumulation in osmotic adjustment in drought-stressed grapevines. Plant Sci 163:361–367

Reape TJ, Molony EM, McCabe PF (2008) Programmed cell death in plants: distinguishing between different modes. J Exp Bot 59:435–444

Robinson E, Kristen U (1982) Membrane flow via the Golgi apparatus of higher plant cells. Int Rev Cytol 77:89–127

Roland JC, Vian B (1991) General preparation and staining of thin sections. In: Hall JL, Hawes C (eds) Electron microscopy of plant cells. Academic, London, pp 1–66

Rost TL, Baum SF, Nichol S (1996) Root apical organization in *Arabidopsis thaliana* ecotype "WS" and a comment on root cap structure. Plant Soil 187:91–95

Sauer M, Paciorek T, Benková E, Friml J (2006) Immunocytochemical techniques for whole-mount in situ protein localization in plants. Nat Protoc 1:98

Sauge-Merle S, Cuine S, Carrier P, Lecomte-Pradines C, Luu DT, Peltier G (2003) Enhanced toxic metal accumulation in engineered bacterial cells expressing *Arabidopsis thaliana*. Appl Environ Microbiol 69:490–494

Scheres B, Benfey P, Dolan L (2002) Root development. In: The *Arabidopsis* book, vol 1. American Society of Plant Biologists, Rockville

Shargil D, Zemach H, Belausov E, Lachman O, Kamenetsky R, Dombrovsky A (2015) Development of a fluorescent in situ hybridization (FISH) technique for visualizing CGMMV in plant tissues. J Virol Methods 223:55–60

Skulachev VP, Bakeeva LE, Chernyak BV et al (2004) Thread-grain transition of mitochondrial reticulum as a step of mitoptosis and apoptosis. Mol Cell Biochem 256/257:341–358

Stadler R, Wright KM, Lauterbach C, Amon G, Gahrtz M, Feuerstein A, Oparka KJ, Sauer N (2005) Expression of GFP-fusions in Arabidopsis companion cells reveals non-specific protein trafficking into sieve elements and identifies a novel post-phloem domain in roots. Plant J 41:319–331

Steer MW (1991) Quantitative morphological analyses. In: Hall JL, Hawes C (eds) Electron microscopy of plant cells. Academic, London, pp 85–104

Stefanowska M, Kuras M, Kacperska A (2002) Low temperature induced modifications in cell ultrastructure and localization of phenolics in winter oilseed rape (Brassica napus L. var. oleifera L.) leaves. Ann Bot 90:637–645

Suksungworn R, Srisombat N, Bapia S, Soun-Udom M, Sanevas N, Wongkantrakorn N, Kermanee P, Vajrodaya S, Duangsrisai S (2017) Coumarins from Haldina cordifolia lead to programmed cell death in giant mimosa: potential bio-herbicides. Pak J Bot 49:1173–1183

Tao L, van Staden J, Cress WA (2000) Salinity induced nuclear and DNA degradation in meristematic of soybean (Glycine max (L.)) roots. Plant Growth Regul 30:49–54

Tian Q, Zhang X, Yang A, Wang T, Zhang W-H (2016) CIPK23 is involved in iron acquisition of Arabidopsis by affecting ferric chelate reductase activity. Plant Sci 246:70–79

Truernit E, Bauby H, Dubreucq B, Grandjean O, Runions J, Barthélémy J, Palauqui J-C (2008) High-resolution whole-mount imaging of three-dimensional tissue organization and gene expression enables the study of phloem development and structure in Arabidopsis. Plant Cell 20:1494–1503

Vaškebová L, Šamaj J, Ovečka M (2017) Single-point ACT2 gene mutation in the Arabidopsis root hair mutant der1–3 affects overall actin organization, root growth and plant development. Ann Bot 00:1–13

Vaughn KC (2006) The abnormal cell plates formed after microtubule disrupter herbicide treatment are enriched in callose. Pest Biochem Physiol 84:63–71

Vaughn KC, Hoffman JC, Hahn MG, Staehelin LA (1996) The herbicide dichlobenil disrupts cell plate formation: inmunogold characterization. Protoplasma 194:117–132

Verma DP (2001) Cytokinesis and building of the cell plate in plants. Annu Rev Plant Physiol Plant Mol Biol 52:751–784

Vladimirov YA, Olenev VI, Suslova TB, Cheremisina ZP (1980) Lipid peroxidation in mitochondrial membranes. Adv Lipid Res 17:173–249

Wiederschain GY (2011) A guide to fluorescent probes and labeling technologies. In: Johnson I, Spence M (eds) The molecular probes handbook, vol 76. Biochemistry, Moscow, pp 1276–1276

Wilson SM, Bacic A (2012) Preparation of plant cells for transmission electron microscopy to optimize immunogold labeling of carbohydrate and protein epitopes. Nat Protoc 7:1716–1727

Yao N, Eisfelder BJ, Marvin J, Greenberg JT (2004) The mitochondrion – an organelle commonly involved in programmed cell death in Arabidopsis thaliana. Plant J 40:596–610

Zhang R, Wise RR, Struck KR, Sharkey TD (2010) Moderate heat stress of Arabidopsis thaliana leaves causes chloroplast swelling and plastoglobule formation. Photosynth Res 105:123–134

Zhao L, Peralta-Videa JR, Ren M, Varela-Ramirez A, Li C, Hernandez-Viezcas JA, Aguilera RJ, Gardea-Torresdey JL (2012) Transport of Zn in a sandy loam soil treated with ZnO NPs and uptake by corn plants: Electron microprobe and confocal microscopy studies. Chem Eng J 184:1–8

Zheng Y, Zhang H, Deng X, Liu J, Chen H (2017) The relationship between vacuolation and initiation of PCD in rice (Oryza sativa) aleurone cells. Sci Rep 7:41245

Zhou J, Wang J, Yu J-Q, Chen Z (2014) Role and regulation of autophagy in heat stress responses of tomato plants. Front Plant Sci 5:174

Zhu T, Rost TL (2000) Directional cell-to-cell communication in the Arabidopsis root apical meristem. III. Plasmodesmata turnover and apoptosis in meristem and root cap cells during four weeks after germination. Protoplasma 213:99–107